Published in final edited form as:
Nat Neurosci. 2008 April ; 11(4): 476–487. doi:10.1038/nn2071.

Synaptic NMDA receptor activity boosts intrinsic antioxidant defences

Sofia Papadia[1,#], **Francesc X. Soriano**[1,#], **Frédéric Léveillé**[1], **Marc-Andre Martel**[1], **Kelly A. Dakin**[2], **Henrik H. Hansen**[3], **Angela Kaindl**[7,8], **Marco Sifringer**[3], **Jill Fowler**[1], **Vanya Stefovska**[3], **Grahame Mckenzie**[4], **Marie Craigon**[5], **Roderick Corriveau**[6], **Peter Ghazal**[5], **Karen Horsburgh**[1], **Bruce A. Yankner**[2], **David J. A. Wyllie**[1], **Chrysanthy Ikonomidou**[3], and **Giles E. Hardingham**[1,9,*]

[1]Centre for Neuroscience Research, University of Edinburgh, Edinburgh EH8 9XD, UK

[2]Department of Pathology, Harvard Medical School, Boston MA 02115, USA

[3]Department of Pediatric Neurology, Technical University Dresden, 01307 Dresden, Germany

[4]Hutchison/MRC Research Centre, MRC Cancer Cell Unit, Cambridge CB2 0XZ, UK

[5]Division of Pathway Medicine, University of Edinburgh, Edinburgh □EH16 4SB,□UK

[6]Coriell Institute for Medical Research, Camden, NJ 08103, USA

[7]Department of Pediatric Neurology, Charité, University Medicine Berlin, 13353 Berlin, Germany

[8]Inserm U676-Paris 7 & Service de Neuropédiatrie, 75019 Paris, France

[9]Royal (Dick) School of Veterinary Studies, Summerhall, Edinburgh EH9 1QH, UK

Abstract

Intrinsic antioxidant defences are important for neuronal longevity. We show that synaptic activity, acting via NMDA receptor (NMDAR) signaling, boosts antioxidant defences through changes to the thioredoxin-peroxiredoxin system. Synaptic activity enhances thioredoxin activity, facilitates the reduction of overoxidized peroxiredoxins, and promotes resistance to oxidative stress. Resistance is mediated by coordinated transcriptional changes: synaptic NMDAR activity inactivates a novel FOXO target gene, the thioredoxin inhibitor Txnip. Conversely, NMDAR blockade upregulates Txnip *in vivo* and *in vitro*, where it binds thioredoxin and promotes vulnerability to oxidative damage. Synaptic activity also up-regulates the peroxiredoxin re-activating genes Sestrin2 and Sulfiredoxin, via C/EBPβ and AP-1 respectively. Mimicking these expression changes is sufficient to strengthen antioxidant defences. Trans-synaptic stimulation of synaptic NMDARs is crucial for boosting antioxidant defences: chronic bath activation of all (synaptic and extrasynaptic) NMDARs induces no antioxidative effects. Thus, synaptic NMDAR activity may influence the progression of pathological processes associated with oxidative damage.

Introduction

Oxidative stress occurs due to an imbalance between production of reactive oxygen species (ROS) and the cell's capacity to neutralize them through its intrinsic antioxidant defences. Neurons are particularly susceptible to oxidative damage due to high levels of ROS

* Correspondence to Giles.Hardingham@ed.ac.uk, Centre for Neuroscience Research, University of Edinburgh, Edinburgh, UK, EH8 9XD. Tel +44 131 6507961, Fax +44 131 6506576..
#These authors made an equal contribution

Europe PMC Funders Author Manuscripts

production (through respiration and metabolism) and relatively low levels of certain antioxidant enzymes, particularly catalase1, 2. Oxidative damage accumulates in normal ageing and plays a role in the pathogenesis of several neurodegenerative diseases as well as acute cerebrovascular disorders1, 2.

Regulation of cellular redox balance depends on the activity of antioxidant systems. Key among these are the thiol reducing systems based round thioredoxin and glutathione, which are important reducers of many oxidative stressors such as peroxides2, 3. The thioredoxin system protects cells against H_2O_2-induced cell death, and its inhibition promotes oxidative stress3. Thioredoxin-overexpressing mice display less oxidative brain damage following ischemia and live longer3.

The thioredoxin system detoxifies peroxides by transferring reducing equivalents from NADPH to peroxides via thioredoxin reductase, thioredoxin and peroxiredoxins (Prxs). Prxs are a family of cytoprotective/antioxidative proteins4-6. The 2-Cys Prxs is the predominant Prx subfamily, comprising Prx I-IV7. These Prxs contain a peroxidatic cysteine residue, oxidized by peroxides to cysteine sulfenic acid (-SOH). Cys-SOH then forms a disulfide bond with the resolving cysteine, which is in turn reduced by thioredoxin7. Sometimes, under increased oxidative stress, Prx-SOH is further oxidized by peroxide to sulfinic (-SO_2H) or sulfonic (-SO_3H) acid, causing inactivation of peroxidase activity8. Prx-$SO_{2/3}H$ is not a substrate for the resolving cysteine and cannot be reduced by thioredoxin. As such, Prx overoxidation to Prx-$SO_{2/3}H$ was thought to be irreversible. Recently, it has been found that Prx-$SO_{2/3}H$ can be reduced back to the catalytically active thiol form by two ATP-dependent reductases, sulfiredoxin8 and sestrin29. It is unknown whether neurons exhibit the capacity to reduce overoxidized Prxs.

There is growing appreciation of the neuroprotective effects of synaptic activity10. In vitro and in vivo studies revealed that part of this activity-dependent neuroprotection is mediated by synaptic NMDAR activity11, 12. NMDAR blockade can trigger widespread neuronal death- an effect which peaks in the first post-natal week in rats13. Newborn neurons of the adult dentate gyrus also have a requirement for NMDAR activity in order to survive14. Where NMDAR blockade does not kill neurons, it can make neurons vulnerable to trauma15.

Despite the importance of neuronal antioxidant defences, little is known about whether they are subject to dynamic regulation, or are a fixed function of neuronal type and age. This is an important question: any regulation could influence biological ageing, or progression of neurodegeneration. Here we study the influence of synaptic activity on the capacity of neurons to deal with oxidative stress. We find that it exerts a profoundly positive effect, mediated by a coordinated program of gene expression changes centred on the thioredoxin-peroxiredoxin system.

Results

Synaptic NMDAR activity boosts antioxidant defences

P6 mice were injected with MK-801 which induced widespread TUNEL-positive cell death in the cortex (Fig. 1a), as was reported for rat brains13. We next determined whether this death was associated with oxidative stress. Following injection of MK-801 or vehicle, cortical proteins were extracted and subjected to 2-D electrophoresis and protein carbonyl levels assayed (a marker of oxidative damage). MK-801 triggered the carbonylation of many cortical proteins (Fig. 1b,c). Thus, suppression of physiological NMDAR activity promotes oxidative damage in the P6-7 cortex. We then investigated the influence of synaptic NMDAR activity on cortical neuronal vulnerability to an oxidative insult (H_2O_2) *in vitro*.

Blockade of spontaneous firing with TTX exacerbated H_2O_2-induced neuronal death (Fig. 1d), as did blockade of spontaneous NMDAR activity by MK-801 (Fig. 1d).

It is likely that most spontaneous NMDAR activity is synaptic, induced by spontaneous firing, and not extrasynaptic (the culture media is glutamate-free). To investigate this we performed analysis of open-channel blockade of NMDARs by MK-801 in current-clamped neurons which revealed a reduction of 43±5% by 5 min which then plateaus (Fig. S1a ('S' denotes supplemental figure)). This current loss is blocked by TTX (Fig. S1b, compare "activity block" with "TTX"), demonstrating that spontaneous NMDAR activity is dependent on action potential (AP) firing, and so likely to be synaptic. To confirm this, we blocked synaptic NMDARs using an established method of holding cells under voltage-clamp in the presence of MK-801, TTX and zero Mg^{2+} 16. Spontaneous release of quanta of glutamate activate synaptic NMDARs which are then blocked by MK-801. As with the previous "activity block" protocol (Fig. S1a), the current that is antagonized using this "quantal block" of synaptic NMDARs plateaus and goes no further (Fig. S1c,d,e). The amount of current blocked using both protocols is similar (Fig. S1b). Furthermore, we performed the "quantal block" protocol after the "activity block" protocol and found no further loss of current (Fig. S1b). Thus, spontaneous NMDAR activity is predominantly synaptic, and dependent on AP firing. Consistent with this, MK-801 + TTX combined did not increase the amount of cell death beyond either drug alone (Fig. S1f), suggesting that TTX and MK-801 are acting via a common pathway that stops spontaneous synaptic NMDAR activity. As expected, MK-801 does not affect underlying firing activity (EPSC frequency is unchanged, Fig. S1g): it is the activation of NMDARs promoted by that underlying activity which is key to the antioxidative effect.

We then used the established method of network disinhibition to enhance synaptic activity, by applying the $GABA_A$ receptor antagonist bicuculline, and the K^+ channel antagonist 4-aminopyridine (which enhances burst frequency, hereafter BiC/4-AP17). BiC/4-AP treatment reduced H_2O_2-induced neuronal death (Fig. 1d), an effect blocked by TTX (Fig. S1h) and also by MK-801 (Fig. 1d). BiC/4-AP treatment triggers activation of synaptic but not extrasynaptic NMDARs17. Therefore the effect of MK-801 in inhibiting the BiC/4-AP-induced neuroprotection is likely to be due to synaptic NMDAR blockade, as has been demonstrated in recent publications17, 18. Note though that during H_2O_2 exposure, there may be some extrasynaptic NMDAR activity due to dying cells releasing glutamate, which would also be blocked by MK-801. However, experiments later firmly implicate synaptic NMDARs as being responsible for the neuroprotective effect observed. As for other potential routes of activity-dependent post-synaptic Ca^{2+} influx: blockade of L-type VGCCs with nifedipine had a small effect on neuroprotection compared to MK-801 (Fig. S1i), while blockade of N-type VGCCs with ω-conotoxin GVIA had no effect (Fig. S1j). Blockade of P/Q-type VGCCs with ω-Agatoxin IVA abolished BiC/4-AP-induced firing (data not shown), consistent with a role for these channels in presynaptic neurotransmitter release.

We corroborated our observations regarding the neuroprotective/antioxidative effects of synaptic NMDAR activity using an alternative measure of cell viability: cellular ATP levels (Fig. 1e). Also, an episode of BiC/4-AP-induced synaptic NMDAR activity that was terminated *before* the addition of H_2O_2 was neuroprotective (Fig. 1f), indicating that long-lasting transcriptional events may be involved. We hypothesized that synaptic activity promotes the reduction/neutralization of cellular ROS following H_2O_2 exposure. We used two fluorogenic ROS probes (2′,7′-dichlorodihydrofluorescein diacetate (H_2DCFDA) and Dihydrorhodamine 123) to detect H_2O_2-induced ROS accumulation (Fig. 1g,h). MK-801-treated neurons contained the highest levels of fluorescent (oxidized) forms of the probes when challenged with H_2O_2, while BiC/4-AP-treated neurons exhibited the least. Thus, H_2O_2-induced ROS accumulation is prevented by synaptic activity. H_2O_2-induced death in

this model is apoptotic: it was prevented by the pan-caspase inhibitor qVD-Oph (fig. S1k). Furthermore, H_2O_2 treatment triggers increased activity of both the initiator caspase 9 and effector caspases 3/7, which was reversed by BiC/4-AP treatment (Fig. S1l).

Overwhelming of the thioredoxin system by oxidative trauma

Of the 2-Cys Prxs, mammalian neurons predominantly express PrxII, III and IV19. Consistent with this, a pan-2-Cys Prx antibody detected 3 bands (Fig. S2a). To identify the bands, we over-expressed PrxII, III and IV in turn and found enrichment of the bottom, middle and upper endogenous band repectively (Fig. S2a), consistent with their theoretical molecular weights.

The existence of overoxidized Prx-$SO_{2/3}$H indicates an overwhelmed thioredoxin-peroxiredoxin system. Western analysis using a Prx-$SO_{2/3}$H-specific antibody revealed that H_2O_2 caused Prx overoxidation in control and MK-801-treated neurons, while BiC/4-AP-treated neurons displayed far less overoxidation (Fig. 2a). MK-801 decreased the effect of BiC/4-AP (Fig. S2b). These differences were not due to BiC/4-AP-induced expression of core components of the thioredoxin-peroxiredoxin system: levels of thioredoxin, thioredoxin reductase and 2-Cys Prxs were unchanged by BiC/4-AP, or by MK-801 (Fig. 2b,c). To find an alternative explanation, we performed microarray expression analysis on neurons experiencing different levels of synaptic NMDAR activity. We searched for genes that were regulated in opposite directions by enhancing/suppressing synaptic NMDAR activity *in vitro* (BiC/4-AP vs. MK-801 treatment), and similarly regulated by NMDAR blockade *in vivo*. We used mouse arrays, since they offered better annotation, and mouse cortical neurons exhibited similar activity-dependent resistance to oxidative stress (data not shown).

Pro-oxidative *Txnip* is suppressed by synaptic activity

Seven genes were induced by BiC/4-AP treatment (in a MK-801-sensitive manner) which were also suppressed by MK-801 *in vitro* and *in vivo* (supplemental table T1). One gene exhibited negative regulation by synaptic NMDAR activity: *Txnip* (thioredoxin interacting protein) which binds thioredoxin, inhibits its activity and promotes vulnerability to oxidative stress3, 20, and was prioritized for further study. We confirmed NMDAR-dependent *Txnip* regulation by q-RT-PCR in mouse (not shown) and rat cortical neurons (Fig. 2d) and by western blot (Fig. 2e). A timecourse revealed *Txnip* expression to be dynamically regulated: both rapidly suppressed by activity, and quickly up-regulated following activity blockade with TTX (Fig. S2c). MK-801 and TTX combined did not induce *Txnip* more than either drug alone (Fig. S2d), consistent with TTX acting by preventing spontaneous synaptic NMDAR activity. Co-immunoprecipitation studies revealed that in MK-801-treated neurons (high Txnip levels), Txnip is bound to thioredoxin (Fig. 2f) which would be expected to inhibit thioredoxin activity. We measured thioredoxin enzyme activity in cell extracts taken under low detergent conditions designed to preserve Txnip-thioredoxin interactions. Enzyme activity in our cultures is almost entirely neuronal: glial cells contribute only 1-2.5 % of thioredoxin activity (see supplemental methods). Consistent with an inhibitory effect of Txnip, extracts from MK-801-treated neurons displayed lower levels of thioredoxin activity than extracts from BiC/4-AP-treated neurons (Fig. 2g), despite equivalent thioredoxin protein levels at 24 and 48 h (Fig. 2b and data not shown). To see whether Txnip renders neurons vulnerable to oxidative stress we over-expressed it in synaptically active neurons, with an eGFP marker to track neuronal fate. >99% of eGFP-expressing cells were NeuN-positive, and <1% were GFAP-positive (data not shown). Expression of Txnip did not alter BiC/4-AP induced bursting (Fig. S3a). By monitoring the neurons before and after H_2O_2 treatment, we found that Txnip expression reduced the antioxidative effects of synaptic activity (Fig. 3a). Consistent with its known function, thioredoxin overexpression was neuroprotective against a H_2O_2 insult (Fig. 3a). We corroborated the effect of Txnip using a

different method of monitoring the viability of transfected neurons: co-expression of a constitutively active luciferase expression construct (Fig. 3b). Thus, Txnip influences neuronal antioxidant defences.

Cortical neuronal death induced by NMDAR blockade is developmentally regulated: at P0 none is observed but by P7 cell-death is widespread13, 21. We found that the coupling of NMDAR blockade to *Txnip* up-regulation *in vivo* is similarly regulated. At P0, MK-801 does not induce an increase in *Txnip*, in contrast to P7 (Fig. 3c), suggesting that Txnip may contribute to cell death at P7. The absence of an effect at P0 could be due to lower NMDAR expression at this stage. We also investigated whether *Txnip* mRNA expression varies with age in humans, and found elevated levels in the cortices from old individuals (81-95 yr) compared to young (25-37 yr, Fig. 3d).

To determine whether suppressing Txnip expression is neuroprotective we investigated the effect of siRNA-mediated knockdown. Validation of *Txnip*-directed siRNA was hampered by the absence of a Txnip antibody which detects endogenous neuronal Txnip by immunohistochemistry, and the fact that at this developmental stage siRNA transfection efficiency is too low to analyze knock-down of endogenous protein by Western blot. Since Txnip protein is sufficiently unstable that suppression of transcription is reflected at the protein level after 24 h (Fig. 2e), we can reasonably assume that effective siRNA is able to knock down endogenous protein levels in a similar timeframe. We expressed rat Txnip in neurons and at 24 h found that co-transfection of two different Txnip-, but not control-siRNA, blocked Txnip expression (Fig. 3e). Neither rat Txnip siRNA impaired expression of transfected human Txnip (Fig. S3c) which contains 2 and 4 nucleotide differences (in central regions) respectively from the corresponding rat sequence.

We found that *Txnip* siRNA did not significantly protect H_2O_2-exposed unstimulated neurons (Fig. 3f) indicating, not surprisingly, that multiple transcriptional changes are needed to mimic the antioxidative effect of synaptic NMDAR activity.

Induction of Prx-$SO_{2/3}$H-reducing genes *Sesn2* and *Srxn1*

To see whether overoxidized Prxs could be reduced in neurons, we applied a brief, high (200 μM) dose of H_2O_2 to induce Prx overoxidation and looked for recovery after H_2O_2 washout. We focussed on PrxII, the major neuronal cytosolic Prx19. Both unstimulated and MK-801-treated neurons exhibited no reduction in Prx-$SO_{2/3}$H 16 h after washout (Fig. 4a). In contrast, BiC/4-AP-treated neurons exhibited a large reduction in post-washout Prx-$SO_{2/3}$H levels (Fig. 4a). Thus, the degree of synaptic activity experienced can determine whether Prx overoxidation is reversible, which may affect the efficacy of H_2O_2 detoxification by the thioredoxin-peroxiredoxin system.

We next studied the transcriptional regulation of the two genes whose products mediate reduction of Prx-$SO_{2/3}$H: sulfiredoxin (*Srxn1*,8) and sestrin2 (*Sesn2*9). BiC/4-AP strongly induced *Srxn1* and *Sesn2* mRNA and protein expression (blocked by MK-801, Fig. 4b,c), offering an explanation for the activity-dependent enhancement of Prx-$SO_{2/3}$H-reducing capacity (Fig. 4a). We hypothesized that up-regulation of *Sesn2* and *Srxn1* may cooperate with the activity-dependent down-regulation of *Txnip* in promoting resistance to oxidative insults. Overexpression of Sesn2 and Srxn1 in a cell-line (HEK293) that is amenable to high efficiency transfection revealed that, following H_2O_2 treatment, Sesn2/Srxn1-coexpressing cells have less Prx-$SO_{2/3}$H than control cells (Fig. S4), in agreement with previous studies9, 22, 23. We then mimicked the three activity-dependent events described above by transfecting expression vectors for *Sesn2* and *Srxn1* as well as *Txnip* siRNA. We found a reduction in cell death following a H_2O_2 insult (Fig. 4d). Expression of Sesn2 and Srxn1 alone afforded variable protection that did not reach significance.

We next performed experiments using siRNA targeted against *Sesn2* and *Srxn1*. Activity-dependent induction of Sesn2 expression was visualized by immunofluorescence, and two siRNAs targeted against *Sesn2* (siRNA(1) and (2)) knocked down expression (Fig. 4e). Validation of *Srxn1*-directed siRNA was hampered by the absence of a Srxn1 antibody which detects endogenous neuronal Srxn1 by immunohistochemistry. Instead, we overexpressed Srxn1 plus a eGFP marker, and analyzed the effectiveness of the siRNA in preventing Srxn1 expression, finding two which worked: siRNA(3) and (4), (Fig. 4f).

We paired the siRNAs (1/3 and 2/4) to test the effect of combined knockdown of *Sesn2* and *Srxn1*. BiC/4-AP-induced protection was diminished in neurons transfected with either pair of siRNAs (Fig. 4g). We also tested the effect of these siRNA pairs on long-lasting protection afforded by a prior episode of synaptic activity (Fig. 1f) and found a similar effect (Fig. 4h). These experiments indicate that the combined changes in Txnip, Sesn2 and Srxn1 expression contribute to the enhancement of intrinsic antioxidant defences mediated by synaptic NMDAR activity.

Txnip is a FOXO target gene

Since *Txnip, Sesn2* and *Srxn1* are novel activity-regulated genes, we wanted to understand how they are regulated. Examination of the *Txnip* promoter revealed a conserved consensus site for the Forkhead box O (FOXO) class of transcription factors (Fig. 5a). FOXOs undergo nuclear export in response to Akt-dependent phosphorylation24 and Akt is activated by synaptic NMDAR activity via phosphatidylinositol-3-kinase (PI3K[18]). Consistent with a role for FOXOs, inhibition of PI3K with LY294002 elevated basal *Txnip* mRNA and protein expression, and blocked activity-dependent suppression of *Txnip* (Fig. 5b). We next cloned the *Txnip* promoter upstream of a luciferase reporter (*Txnip*-Luc) and introduced a mutation into the putative FOXO binding site (*Txnip*(mut)-Luc). *Txnip*-Luc exhibited the expected activity-dependent suppression (Fig. 5c), while *Txnip*(mut)-Luc exhibited lower basal activity and did not undergo activity-dependent suppression (Fig. 5c). Overexpression of the major neuronal FOXOs, FOXO1 or FOXO3a, enhanced *Txnip*-Luc promoter activity but failed to activate *Txnip*(mut)-Luc (Fig. 5d). Thus, *Txnip* contains a functional FOXO site which mediates activity-dependent inactivation of the promoter. Moreover, we found that BiC/4-AP treatment triggered PI3K-dependent FOXO1 phosphorylation (Fig. 5e) and nuclear export (Fig. 5f). In contrast, MK-801 enhanced nuclear localisation of FOXO1 (Fig. 5f). A mutant FOXO with its Akt phosphorylation sites mutated (FOXO-ADA[25]) did not undergo activity-dependent export (data not shown). Chromatin-IP experiments revealed that endogenous FOXO1 associates with the *Txnip* promoter in MK-801-treated neurons more strongly than in BiC/4-AP-treated neurons (Fig. 5g,h). As a negative control, chromatin-IP with a phospho-FOXO1 antibody failed to immunoprecipitate the *Txnip* promoter (Fig. 5h). Consistent with the intermediate nature of the untreated neurons with regard to *Txnip* expression and FOXO localisation, they exhibited variable FOXO promoter occupancy: sometimes resembling MK-801-treated neurons and sometimes BiC/4-AP-treated neurons (Fig. 5h left vs. right). These data support a model whereby synaptic activity turns off *Txnip* ranscription by inducing the PI3K-Akt pathway, triggering FOXO phosphorylation, dissociation from the *Txnip* promoter and export from the nucleus.

Sesn2 is a C/EBP target gene

We created a *Sesn2*-Luciferase reporter, which was activated by BiC/4-AP-induced NMDAR activity (Fig. S5a). Deletion analysis identified the activity-inducible region between -494 and -107 relative to the transcription start site (Fig. 6a). Further deletions revealed that inducibility was conferred by 2 regions: -378 to -249 and -249 to -107 (data not shown). *In silico* analysis revealed a potential binding site for the transcription factor CCAAT enhancer binding protein (C/EBP) in each of these regions. Moreover, expression

of an interfering mutant of C/EBP, ΔC/EBP26, inhibited activity-dependent induction of *Sesn2*-Luc (Fig. 6b). Mutation of the proximal putative C/EBP site impaired activity-dependent induction of *Sesn2*-Luc (Fig. 6c), while mutation of both sites abolished induction (Fig. 6c). Thus, induction of *Sesn2* by synaptic activity is mediated largely by C/EBP.

Transcription of the *Cebpb* gene (but not *Cebpa*) is induced by BiC/4-AP stimulation (Fig. 6d, and data not shown), raising the possibility that this new expression may be important for *Sesn2* induction. Consistent with this, Sesn2 is not an immediate early gene: it was not induced at 1 h (Fig. S5b), and induction at 4 h was severely inhibited by the protein synthesis inhibitor cycloheximide (Fig. S5b). C/EBPβ is a CREB-regulated immediate early gene27, induction of which is *not* inhibited by cycloheximide (Fig. S5c). The rapid induction at 1 h contrasts with the slower induction of *Sesn2*, consistent with the predominantly delayed-response nature of *Sesn2* induction.

Srxn1 is an AP-1 target gene

We created a *Srxn1*-Luciferase reporter which was activated by BiC/4-AP-induced NMDAR activity (Fig. S5a). Deletion analysis identified the activity-inducible region between -645 and -234 relative to the translation start site (Fig. 6e). Analysis of this region revealed two putative AP-1 sites (TGAGTCA). Ca^{2+} signaling is known to activate AP-1 family members, confirmed by our observation that BiC/4-AP stimulation activates a heterologous AP-1 reporter 6.1 ± 0.61 fold (n=4). Overexpression of AP-1 (c-fos and c-jun) strongly induced activity of the *Srxn1* reporter, which was impaired when either putative AP-1 site was mutated, and abolished in the double mutant (Fig. 6f). Moreover, mutation of either site significantly reduced activity-dependent induction of the *Srxn1* reporter construct, and the double mutation abolished induction (Fig. 6g). Thus, *Srxn1* is activated via AP-1 sites in its promoter.

Extrasynaptic NMDARs fail to boost antioxidant defences

Trans-synaptic activation of synaptic NMDARs is anti-apoptotic, however, chronic activation of all (synaptic and extrasynaptic) NMDARs by bath application of glutamate/NMDA is not17. Moreover, synaptic vs. bath activation of NMDARs promote very different transcriptional responses28. We tested whether trans-synaptic activation of synaptic NMDARs is critical for NMDAR-dependent antioxidative effects, or whether bath application of glutamate will suffice. We bath-applied a range of glutamate doses (up to the toxicity threshold: 20 μM) in the presence of TTX to ensure that there was no preferential activation of synaptic NMDARs, as can occur29. Stimulations were compared to control (TTX only).

We first analysed bath-glutamate signaling to Akt, FOXO export, and Txnip suppression. Sustained glutamate exposure only triggered transient Akt activation (Fig. 7a) and weak FOXO export (Fig. 7b). Suppression of *Txnip* expression was poor compared to BiC/4-AP stimulation (Fig. 7c). Also, no dose of bath glutamate induced either *Sesn2* or *Srxn1* appreciably (Fig. 7d,e) nor was there significant induction of *Sesn2*'s activator, *Cebpb* (Fig. 7f). Consistent with this, glutamate did not promote the reduction of overoxidized Prxs (Fig. 7g,h), nor induce protection against H_2O_2-induced death (Fig. 7i). Thus, the strong antioxidative effect of NMDAR signaling is restricted to the trans-synaptic activation of synaptic NMDARs, and is not a pre-conditioning-type effect in response to sub-toxic glutamate exposure.

We next investigated whether these differences are due to NR2 subunit differences between synaptic and extrasynaptic NMDARs, since NR2A-containing NMDARs may be enriched at

synaptic locations30 and signal to neuroprotection more effectively than NR2B-containing NMDARs31. Both whole-cell NMDAR currents and extrasynaptic NMDAR currents (analyzed by blocking synaptic NMDARs with the "quantal block" protocol, Fig. S1c) were blocked by 70% by the NR2B antagonist ifenprodil (Fig. 8a). Ifenprodil does not completely block responses even when mediated exclusively by NR2B-containing NMDARs (around 80 % is achieved32). Thus, synaptic and extrasynaptic NMDARs are overwhelmingly and equally NR2B-dominated, a likely consequence of the relatively early developmental stage under study.

We hypothesized that both harmful and protective consequences of NMDAR activation in these neurons would be inhibited by NR2B antagonists. Both ifenprodil and Ro 25-6981 protected neurons from cell death induced by a toxic dose of NMDA (50 μM, Fig. 8b). NR2B antagonists also impaired protective signaling by trans-synaptic activation of synaptic NMDARs: ifenprodil and Ro 25-6981 exacerbated neuronal death by H_2O_2 (Fig. 8c), caused an up-regulation of *Txnip* (Fig. 8d), reduced BiC/4-AP induced protection against H_2O_2-induced death (Fig. 8e) and reduced signaling to *Sesn2* and *Srxn1* activation (Fig. 8f). Thus, differences in the effect of synaptic stimulation vs. bath application of agonist are unlikely to be due to large, clear-cut differences in NR2 subunit composition at synaptic and extrasynaptic sites. However, we cannot rule out a role for NR2A-containing NMDARs at the synapse-this would require analyses of NR2A-null neurons.

Memantine is an open channel blocker with a fast off-rate. Its uncompetitive nature results in an effective blockade of chronic NMDAR activity caused by bath-applied glutamate33. However, due to its fast off-rate and voltage-dependent binding properties, memantine does not substantially interfere with normal synaptic NMDAR activity by accumulating in the channel33. In the context of this study, memantine appears suited to the sparing of the antioxidative effects of trans-synaptic activation of synaptic NMDARs, while blocking chronic activation of NMDARs by low level glutamate which does not enhance antioxidant defences (Fig. 7i).

Memantine (at 5 μM or 10 μM) blocks NMDAR-dependent neuronal death induced by 50 μM NMDA (Fig. 8g). However, it does not interfere with trans-synaptic NMDAR-dependent activation of antioxidant defenses: unlike MK-801, memantine does not exacerbate H_2O_2-induced death (Fig. 8h) nor promote nuclear localisation of FOXOs (Fig. 8i) or *Txnip* expression (Fig. 8j), and does not interfere with synaptic activity-dependent signaling to *Sesn2* and *Srxn1* activation (Fig. 8k,l) nor *Txnip* suppression (Fig. 8m), nor activity-dependent neuroprotection against H_2O_2 (Fig. 8n). We also assessed the effects of memantine administration *in vivo* at a dose (20 $mgkg^{-1}$) consistently shown to be therapeutically active in protecting against ischemic insults 34 and known to result in brain concentrations of memantine similar to those used in our *in vitro* experiments35. Unlike MK-801, memantine injection does not cause neuronal apoptosis in the P7 cortex: no death was observed either by TUNEL-staining (Fig. 8o) or Fluorojade staining, which labels degenerating neurons irrespective of mechanism of death (data not shown). The differential effects of MK-801 and memantine emphasize that trans-synaptic stimulation of synaptic NMDARs is important for boosting antioxidant defences and that blockade of synaptic NMDARs boosts vulnerability to oxidative stress *in vitro* and *in vivo*.

Overoxidation of peroxiredoxins by ischemia/reperfusion

We wanted to determine whether the thioredoxin system becomes overwhelmed in an *in vivo* model of neuronal death. We chose ischemia/reperfusion as a model to study, since it is associated with an acute wave of oxidative damage that affects a significant population of neurons and is implicated in the pathological process1. We subjected adult mice to 60 min

MCAO and examined extracts from cortical regions at 4 h post-reperfusion, which is prior to development of the infarct.

Increased Prx-$SO_{2/3}$H formation in the MCA territory (cortex and striatum) following ischemia/reperfusion is evident, compared to equivalent samples from the sham-operated individuals (Fig. 9). The profile of overoxidation is subtly different from that of *in vitro* H_2O_2 treatment: PrxIII is overoxidized to a greater extent by ischemia/reperfusion than by H_2O_2 treatment. Thus, Prx-$SO_{2/3}$H formation does occur *in vivo* in response to brain insult, indicating that the thioredoxin-peroxiredoxin system is overwhelmed. This lends added relevance to our findings concerning the regulation of genes whose products can influence this system.

Discussion

We have demonstrated that neuronal antioxidative defences are subject to activity-dependent enhancement, mediated by synaptic NMDAR signaling. A coordinated program of gene expression changes with a net antioxidative effect underlies this enhancement. The changes described centre on the thioredoxin-peroxiredoxin system, and involve hitherto uncharacterized activity-regulated genes.

Txnip promotes oxidative stress and cell death

Txnip interacts with the reduced form of thioredoxin, inhibits its biochemical activity and sensitizes a variety of cell types to H_2O_2-induced death3, 20. Txnip is implicated in the pathogenesis of diabetes: it is up-regulated in the vasculature and pancreatic beta cells of diabetic rats and is induced by hyperglycaemia in both systems, promoting oxidative stress20, 36. Txnip plays a role in oncology: it is proposed to suppress tumour cell growth and metastasis, and reduced levels have been observed in a variety of cancers3. Txnip's influence on neuronal vulnerability to oxidative stress is consistent with its role as a pro-oxidative gene in non-neuronal systems.

Studies on transcriptional control by synaptic Ca^{2+} signals focus almost exclusively on up-regulated genes. Results here concerning the regulation of *Txnip* expression demonstrate that gene inactivation must also be considered. Our findings that *Txnip* is regulated by FOXOs adds to our knowledge of FOXO-regulated pro-death genes, which thus far have focussed mainly on *Bim* and *FasL*24, 37.

Peroxiredoxins are cytoprotective antioxidant enzymes

Prxs are a family of thiol-based antioxidants with cytoprotective effects in the face of oxidative insults. PrxII protects cortical neurons against Aβ toxicity38 and oxygen-glucose deprivation 39. Interfering with PrxII expression renders neuroblastoma cells vulnerable to oxidative stress5, and renders cortical neurons vulnerable to MPP^+ 6. PrxIII protects hippocampal neurons against excitotoxicity4.

Low reported catalytic rates for Prxs led to the suggestion that Prxs would not be able to compete with catalase or glutathione peroxidases for cellular peroxide, despite evidence of the antioxidative properties of Prxs. This apparent paradox was due to an underestimation of peroxidase rates of mammalian PrxII, as a result of their indirect calculation by measuring NADPH oxidation rates which measure regeneration by the thioredoxin system. When peroxide levels are high, it is clear that the thioredoxin system cannot keep up. In fact, when rates of mammalian Prx were measured directly40 they were found to be 100 fold greater than previously thought, similar to rates recently found in PrxI and II from *S. cerevisiae*41. Since Prxs are relatively abundant, they are likely to play an important antioxidant role in mammalian *in vivo* systems.

Thus, molecular events that render Prxs inactive *in vivo* in pathological scenarios may contribute to disease progression. We observe Prx-inactivating Prx-$SO_{2/3}H$ formation following cerebral ischemia *in vivo* (Fig. 9), but this is not the only way by which Prxs can be inhibited: The enzymic activity of PrxII can be impaired by cdk5-mediated phosphorylation6 and by nitrosylation42, both of which occur in Parkinson's Disease6, 42.

Re-activation of Prx-$SO_{2/3}H$ by Sulfiredoxin and Sestrin2

Sulfiredoxin was initially characterized in yeast43 and then in mammalian cells 8 and acts by catalysing the ATP-dependent formation of a sulfinic acid phosphoric ester on Prx8 which is then reduced by thiol equivalents such as thioredoxin. The mechanism of ATP-dependent Sesn2 is unknown9. The capacity of neurons to reduce inactive Prx-$SO_{2/3}H$ was hitherto unknown, and our findings show that active neurons have a far greater capacity for this than inactive neurons, and are associated with high levels of *Srxn1* and *Sesn2*. This is the first time that Prx-$SO_{2/3}H$ reducing activity has been found to be signal-dependent. Given the widespread expression of these genes, this raises the question as to whether the Prx-SO_2H reduction process is signal-inducible *in vivo*. For example, ischemic preconditioning is associated with activation of AP-144 which could therefore result in up-regulation of Srxn1 expression and reduce Prx-$SO_{2/3}H$ formation that occurs following ischemia (Fig. 9).

Activity-dependent regulation of antioxidant defences

It is not clear why synaptic activity, acting via Ca^{2+} signaling, should act to boost antioxidant defences. One possibility is to protect against increased ROS generation: electrical activity and its downstream physiological consequences are expensive energetically and metabolically. ROS are generated as a by-product of respiration and many metabolic pathways, so the regulation of antioxidant defences may be a homeostatic mechanism to ensure the correct redox balance in the neuron. However, results described here show that the effects of synaptic activity go beyond protecting against increased endogenous ROS production, since it renders neurons resistant to an exogenously applied insult.

An implication of our work is that a neuron's lifelong pattern of activity may influence its accumulation of oxidative damage and ultimately its longevity during ageing, or affect the progression of pathological processes associated with oxidative damage such as AD or PD. This raises the question as to whether altered patterns of neuronal activity *in vivo*, in response to changes in behaviour or environment, can alter neuronal antioxidative capacity. Rodent environmental enrichment (EE) is neuroprotective and modulates onset and severity of models of AD and Huntington's disease, while in humans, a cognitively stimulating lifestyle may reduce risk of AD and PD45, 46. It is an intriguing possibility that EE may, through altered or increased patterns of neuronal activity, result in increased antioxidant defences in those brain regions that are more intensively used. We find that only 5 minutes of BiC/4-AP induced burst activity significantly induce *Srxn1* expression (by 40%, Fig. S6a) and induce down-regulation of *Txnip* (by 60%, Fig. S6b), raising the possibility that modest episodes of elevated activity *in vivo* may trigger significant changes.

NMDAR blockade can trigger widespread neuronal death- an effect which peaks in the first post-natal weeks in rats. NMDAR blockade does not kill adult neurons outright13. Consistent with this, carbonyl assay of cortical proteins from MK-801 injected adult mice (Fig. S7) revealed no significant increases in carbonylation of any proteins (in sharp contrast to the P7 cortex, Fig. 1b) although there was a trend towards an increase in carbonylation in several spots. NMDAR blockade in the adult CNS can exacerbate death in response to metabolic inhibition or traumatic brain injury 11, 15. The borderline effects of MK-801 in

the adult cortex with regard to oxidative stress (Fig. S7) may translate to more substantial increases when the brain is subject to an additional trauma, and contribute to the increased neuronal death observed 11, 15.

The growing understanding of the neuroprotective effects of physiological synaptic NMDAR activity, coupled with its established role in synaptic plasticity, suggests that global NMDAR antagonism may not be appropriate as a anti-excitotoxic or anti-apoptotic therapeutic strategy12, 47. Memantine is a NMDAR antagonist approved for AD, and unlike conventional antagonists, has properties suited to sparing trans-synaptic activation of synaptic NMDARs, while blocking continuous low level NMDAR activation by chronic glutamate exposure33. This enhancement of physiological signal over pathological noise is thought to improve plastic processes at the synapse and prevent apoptosis caused by chronic low level activation of NMDARs33. In our hands, memantine is able to prevent NMDAR-dependent excitotoxic cell death, while not inhibiting the antioxidative effects of trans-synaptic activation of synaptic NMDARs. These findings are consistent with memantine's clinically tolerated mechanism of action33.

The ageing human brain is associated with an accumulation of oxidative damage2. Elevated levels of *Txnip* expression in the ageing human cortex (Fig. 3d) may be a consequence of lowered levels of activity and could conceivably influence vulnerability to oxidative stress. The situation is exacerbated in AD sufferers, where *Txnip* levels are further elevated48, as are levels of FOXO1 and FOXO3a mRNA48, activators of *Txnip* (Fig. 5). Whether any of these expression changes represents a contributing factor to pathogenesis, or merely an epiphenomenon, is not clear. Nor is it clear whether expression of *Srxn1* or *Sesn2* are altered in neurodegenerative diseases. An understanding of the signals and genes that control neuronal antioxidant defences may point the way to therapeutic strategies aimed at slowing neurodegeneration in a variety of disorders associated with oxidative damage.

Experimental Procedures

See Supplemental Methods file (SuppMethods.doc) for further information.

Neuronal cultures, stimulation, and the induction of oxidative stress

Cortical rat neurons were cultured as described 18 from E21 rats or E17 mouse pups in Neurobasal-A medium and B27 (Invitrogen). Stimulations and transfections (Lipofectamine 2000, Invitrogen) were done at DIV8-10 after transferring neurons into trophically-deprived medium 18. Action potential bursting was induced by treatment with 50 μM bicuculline, plus 250 μM 4-aminopyridine (Sigma) to enhance burst frequency. Stimulations were initiated 12 h prior to the application of an oxidative insult. Neurons were fixed after a further 24 h and subjected to DAPI staining and cell death quantified by counting (blind) the number of apoptotic nuclei as a percentage of the total. For details of analysis of peroxide-induced ROS accumulation and caspase activity, see supplemental methods.

Electrophysiological recording and analysis

Currents were recorded (at 21±2°C) using an Axopatch-1C amplifier (Molecular Device, Union City, CA). Data were digitized and analyzed using WinEDR v6.1 software (John Dempster, University of Strathclyde, UK). Neurons were voltage-clamped at -70 mV, and recordings were rejected if the holding current was >-100 pA or if the series resistance drifted by >20% of its initial value (<35 MΩ). See supplemental methods for details of solutions, drugs and of "activity block" and "quantal block" protocols

Gene expression analysis by qPCR and microarray

For qPCR, cDNA was synthesized from 1-3 μg RNA (extracted using Qiagen Rneasy kit) using the Stratascript QPCR cDNA Synthesis kit and qPCR performed in an Mx3000P QPCR System (Stratagene) using Brilliant SYBR Green QPCR Master Mix. For detailed protocols and primer sequences, see supplemental methods. For microarray-based expression analysis, total RNA was quality-confirmed on RNA 6000 Nanochips in the Agilent 2100 Bioanalyzer. Purified biotinylated target cRNA was produced (see supplemental methods) and hybridized to Mouse Genome 430A plus 2.0 microarrays (Affymetrix). After hybridization, the arrays were washed and scanned (Genechip Scanner 3000, Affymetrix). Expression was calculated using the robust multiarray average algorithm implemented in the Bioconductor (http://www.bioconductor.org) extensions to the R statistical programming environment.

In vivo procedures

In vivo MK-801 and memantine administration, TUNEL histology, and protein carbonyl assay of extracted proteeins were all performed using established techniques. In vivo focal cerebral ischemia was performed on adult male C57Bl/6J mice under an appropriate Home Office Licence. See supplemental methods section for details of all *in vivo* procedures.

Other experimental procedures and materials

Neuronal transfections, following the fate of transfected cells, luciferase assays, immunofluorescencent staining, western blotting, chromatin immunoprecipitation, co-immunoprecipitation and thioredoxin enzyme assays all involved standard protocols (see supplemental methods section for these and information on plasmids, siRNA and antibodies).

Supplementary Material

Refer to Web version on PubMed Central for supplementary material.

Acknowledgments

We thank Peter Brophy for critically reading the manuscript, and acknowledge Janine Stuwe's assistance. We also thank David Bennett and the Rush Alzheimer's Disease Center (NIH grant P30AG10161) for providing some of the brain samples used in this study, and thank Domenico Accili, Hilmar Bading, Jean-Claude Chambard, Richard Lee, Charles Vinson, George Wilding and Junji Yodoi for plasmids. This work was funded by the Wellcome Trust, a Royal Society University Research Fellowship (GH), Medical Research Scotland, Tenovus Scotland, the BBSRC, Sanitaetsrat Dr. Emil Alexander Huebner and Gemahlin-Stiftung and a Rahel Hirsch scholarship from the Humboldt University Berlin.

References

1. Mariani E, Polidori MC, Cherubini A, Mecocci P. Oxidative stress in brain aging, neurodegenerative and vascular diseases: an overview. J Chromatogr B Analyt Technol Biomed Life Sci. 2005; 827:65–75.
2. Halliwell B. Oxidative stress and neurodegeneration: where are we now? J Neurochem. 2006; 97:1634–1658. [PubMed: 16805774]
3. Yoshida T, Nakamura H, Masutani H, Yodoi J. The involvement of thioredoxin and thioredoxin binding protein-2 on cellular proliferation and aging process. Ann N Y Acad Sci. 2005; 1055:1–12. [PubMed: 16387713]
4. Hattori F, Murayama N, Noshita T, Oikawa S. Mitochondrial peroxiredoxin-3 protects hippocampal neurons from excitotoxic injury in vivo. J Neurochem. 2003; 86:860–868. [PubMed: 12887684]
5. Sanchez-Font MF, et al. Peroxiredoxin 2 (PRDX2), an antioxidant enzyme, is under-expressed in Down syndrome fetal brains. Cell Mol Life Sci. 2003; 60:1513–1523. [PubMed: 12943237]

6. Qu D, et al. Role of Cdk5-mediated phosphorylation of Prx2 in MPTP toxicity and Parkinson's disease. Neuron. 2007; 55:37–52. [PubMed: 17610816]
7. Wood ZA, Schroder E, Robin Harris J, Poole LB. Structure, mechanism and regulation of peroxiredoxins. Trends Biochem Sci. 2003; 28:32–40. [PubMed: 12517450]
8. Rhee SG, Jeong W, Chang TS, Woo HA. Sulfiredoxin, the cysteine sulfinic acid reductase specific to 2-Cys peroxiredoxin: its discovery, mechanism of action, and biological significance. Kidney Int Suppl. 2007:S3–8. [PubMed: 17653208]
9. Budanov AV, Sablina AA, Feinstein E, Koonin EV, Chumakov PM. Regeneration of peroxiredoxins by p53-regulated sestrins, homologs of bacterial AhpD. Science. 2004; 304:596–600. [PubMed: 15105503]
10. Mennerick S, Zorumski CF. Neural activity and survival in the developing nervous system. Mol Neurobiol. 2000; 22:41–54. [PubMed: 11414280]
11. Olney JW, et al. Drug-induced apoptotic neurodegeneration in the developing brain. Brain Pathol. 2002; 12:488–498. [PubMed: 12408236]
12. Papadia S, Hardingham GE. The Dichotomy of NMDA Receptor Signaling. Neuroscientist. 2007
13. Ikonomidou C, et al. Blockade of NMDA receptors and apoptotic neurodegeneration in the developing brain. Science. 1999; 283:70–74. [PubMed: 9872743]
14. Tashiro A, Sandler VM, Toni N, Zhao C, Gage FH. NMDA-receptor-mediated, cell-specific integration of new neurons in adult dentate gyrus. Nature. 2006; 442:929–933. [PubMed: 16906136]
15. Ikonomidou C, Stefovska V, Turski L. Neuronal death enhanced by *N*-methyl-D-aspartate antagonists. Proc Natl Acad Sci U S A. 2000; 97:12885–12890. [PubMed: 11058158]
16. Nakayama K, Kiyosue K, Taguchi T. Diminished neuronal activity increases neuron-neuron connectivity underlying silent synapse formation and the rapid conversion of silent to functional synapses. J Neurosci. 2005; 25:4040–4051. [PubMed: 15843606]
17. Hardingham GE, Fukunaga Y, Bading H. Extrasynaptic NMDARs oppose synaptic NMDARs by triggering CREB shut-off and cell death pathways. Nat Neurosci. 2002; 5:405–414. [PubMed: 11953750]
18. Papadia S, Stevenson P, Hardingham NR, Bading H, Hardingham GE. Nuclear Ca2+ and the cAMP response element-binding protein family mediate a late phase of activity-dependent neuroprotection. J Neurosci. 2005; 25:4279–4287. [PubMed: 15858054]
19. Jin MH, et al. Characterization of neural cell types expressing peroxiredoxins in mouse brain. Neurosci Lett. 2005; 381:252–257. [PubMed: 15896479]
20. Schulze PC, et al. Hyperglycemia promotes oxidative stress through inhibition of thioredoxin function by thioredoxin-interacting protein. J Biol Chem. 2004; 279:30369–30374. [PubMed: 15128745]
21. Adams SM, de Rivero Vaccari JC, Corriveau RA. Pronounced cell death in the absence of NMDA receptors in the developing somatosensory thalamus. J Neurosci. 2004; 24:9441–9450. [PubMed: 15496680]
22. Chang TS, et al. Characterization of mammalian sulfiredoxin and its reactivation of hyperoxidized peroxiredoxin through reduction of cysteine sulfinic acid in the active site to cysteine. J Biol Chem. 2004; 279:50994–51001. [PubMed: 15448164]
23. Woo HA, et al. Reduction of cysteine sulfinic acid by sulfiredoxin is specific to 2-cys peroxiredoxins. J Biol Chem. 2005; 280:3125–3128. [PubMed: 15590625]
24. Brunet A, et al. Akt promotes cell survival by phosphorylating and inhibiting a Forkhead transcription factor. Cell. 1999; 96:857–868. [PubMed: 10102273]
25. Nakae J, Barr V, Accili D. Differential regulation of gene expression by insulin and IGF-1 receptors correlates with phosphorylation of a single amino acid residue in the forkhead transcription factor FKHR. Embo J. 2000; 19:989–996. [PubMed: 10698940]
26. Olive M, Williams SC, Dezan C, Johnson PF, Vinson C. Design of a C/EBP-specific, dominant-negative bZIP protein with both inhibitory and gain-of-function properties. J Biol Chem. 1996; 271:2040–2047. [PubMed: 8567657]
27. Niehof M, Manns MP, Trautwein C. CREB controls LAP/C/EBP beta transcription. Mol Cell Biol. 1997; 17:3600–3613. [PubMed: 9199295]

28. Zhang SJ, et al. Decoding NMDA Receptor Signaling: Identification of Genomic Programs Specifying Neuronal Survival and Death. Neuron. 2007; 53:549–562. [PubMed: 17296556]
29. Soriano FX, et al. Preconditioning doses of NMDA promote neuroprotection by enhancing neuronal excitability. J Neurosci. 2006; 26:4509–4518. [PubMed: 16641230]
30. Steigerwald F, et al. C-Terminal truncation of NR2A subunits impairs synaptic but not extrasynaptic localization of NMDA receptors. J Neurosci. 2000; 20:4573–4581. [PubMed: 10844027]
31. Liu Y, et al. NMDA receptor subunits have differential roles in mediating excitotoxic neuronal death both in vitro and in vivo. J Neurosci. 2007; 27:2846–2857. [PubMed: 17360906]
32. Tovar KR, Westbrook GL. The incorporation of NMDA receptors with a distinct subunit composition at nascent hippocampal synapses *in vitro*. The Journal of Neuroscience. 1999; 19:4180–4188. [PubMed: 10234045]
33. Chen HS, Lipton SA. The chemical biology of clinically tolerated NMDA receptor antagonists. J Neurochem. 2006; 97:1611–1626. [PubMed: 16805772]
34. Seif el Nasr M, Peruche B, Rossberg C, Mennel HD, Krieglstein J. Neuroprotective effect of memantine demonstrated in vivo and in vitro. Eur J Pharmacol. 1990; 185:19–24. [PubMed: 2226632]
35. Wesemann W, Schollmeyer JD, Sturm G. Distribution of memantine in brain, liver, and blood of the rat. Arzneimittelforschung. 1982; 32:1243–1245. [PubMed: 6891224]
36. Minn AH, Hafele C, Shalev A. Thioredoxin-interacting protein is stimulated by glucose through a carbohydrate response element and induces beta-cell apoptosis. Endocrinology. 2005; 146:2397–2405. [PubMed: 15705778]
37. Gilley J, Coffer PJ, Ham J. FOXO transcription factors directly activate bim gene expression and promote apoptosis in sympathetic neurons. J Cell Biol. 2003; 162:613–622. [PubMed: 12913110]
38. Yao J, et al. Interaction of amyloid binding alcohol dehydrogenase/Abeta mediates up-regulation of peroxiredoxin II in the brains of Alzheimer's disease patients and a transgenic Alzheimer's disease mouse model. Mol Cell Neurosci. 2007; 35:377–382. [PubMed: 17490890]
39. Boulos S, Meloni BP, Arthur PG, Bojarski C, Knuckey NW. Peroxiredoxin 2 overexpression protects cortical neuronal cultures from ischemic and oxidative injury but not glutamate excitotoxicity, whereas Cu/Zn superoxide dismutase 1 overexpression protects only against oxidative injury. J Neurosci Res. 2007; 85:3089–3097. [PubMed: 17663478]
40. Peskin AV, et al. The high reactivity peroxiredoxin 2 with H2O2 is not reflected in its reaction with other oxidants and thiol reagents. J Biol Chem. 2007
41. Ogusucu R, Rettori D, Munhoz DC, Netto LE, Augusto O. Reactions of yeast thioredoxin peroxidases I and II with hydrogen peroxide and peroxynitrite: rate constants by competitive kinetics. Free Radic Biol Med. 2007; 42:326–334. [PubMed: 17210445]
42. Fang J, Nakamura T, Cho DH, Gu Z, Lipton SA. S-nitrosylation of peroxiredoxin 2 promotes oxidative stress-induced neuronal cell death in Parkinson's disease. Proc Natl Acad Sci U S A. 2007; 104:18742–18747. [PubMed: 18003920]
43. Biteau B, Labarre J, Toledano MB. ATP-dependent reduction of cysteine-sulphinic acid by S. cerevisiae sulphiredoxin. Nature. 2003; 425:980–984. [PubMed: 14586471]
44. Kapinya K, Penzel R, Sommer C, Kiessling M. Temporary changes of the AP-1 transcription factor binding activity in the gerbil hippocampus after transient global ischemia, and ischemic tolerance induction. Brain Res. 2000; 872:282–293. [PubMed: 10924710]
45. Young D, Lawlor PA, Leone P, Dragunow M, During MJ. Environmental enrichment inhibits spontaneous apoptosis, prevents seizures and is neuroprotective. Nature Medicine. 1999; 5:448–453.
46. Spires TL, Hannan AJ. Nature, nurture and neurology: gene-environment interactions in neurodegenerative disease. FEBS Anniversary Prize Lecture delivered on 27 June 2004 at the 29th FEBS Congress in Warsaw. Febs J. 2005; 272:2347–2361. [PubMed: 15885086]
47. Muir KW. Glutamate-based therapeutic approaches: clinical trials with NMDA antagonists. Curr Opin Pharmacol. 2006; 6:53–60. [PubMed: 16359918]

48. Blalock EM, et al. Incipient Alzheimer's disease: microarray correlation analyses reveal major transcriptional and tumor suppressor responses. Proc Natl Acad Sci U S A. 2004; 101:2173–2178. [PubMed: 14769913]

49. Lu T, et al. Gene regulation and DNA damage in the ageing human brain. Nature. 2004; 429:883–891. [PubMed: 15190254]

50. Osada S, Yamamoto H, Nishihara T, Imagawa M. DNA binding specificity of the CCAAT/enhancer-binding protein transcription factor family. J Biol Chem. 1996; 271:3891–3896. [PubMed: 8632009]

Europe PMC Funders Author Manuscripts

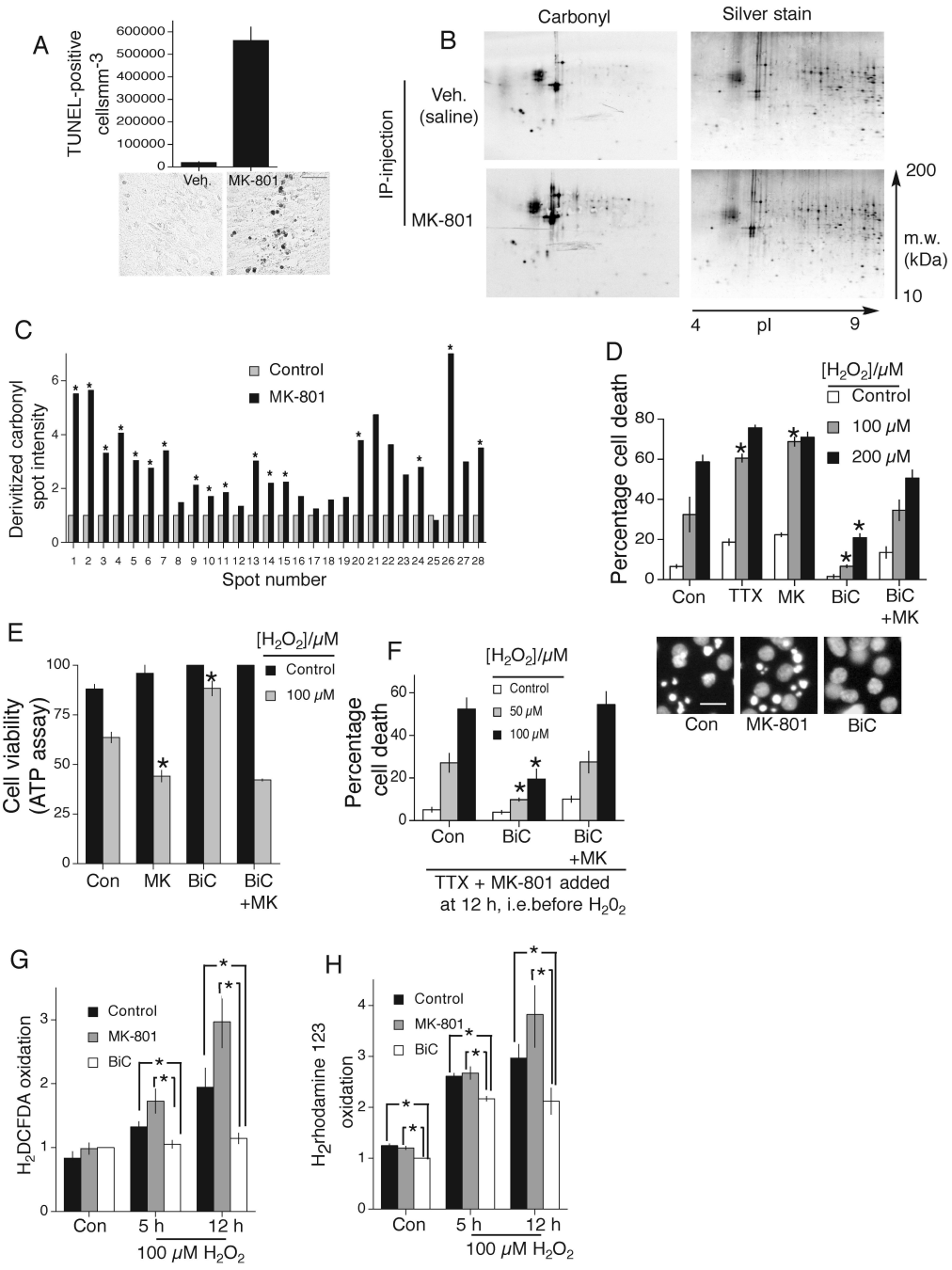

Fig. 1. Synaptic NMDAR activity promotes resistance to oxidative insults and prevents ROS accumulation

A) TUNEL-positive apoptosis in the cortex of P7 mice subjected to IP-injection of MK-801 at P6 (exposure for 24 h). Quantitation (upper) and representative sections (lower-scale bar 200 μm). B,C) Analysis of carbonyl content of 2-D separated proteins from the cortices of P7 mice subjected to IP-injection of MK-801. Blotted 2-DE gels were stained with silver staining to reveal protein spots (right). C) Comparison of intensity of representative protein spots *$p<0.05$ (n=6) 2-tailed T-test (in this and subsequent cases unless stated). D) Cell death due to 24 h H_2O_2 insult in the face of the indicated treatments, applied 12 h before insult. BiC/4-AP stimulation is labelled as “BiC” in this and subsequent figures. (Lower)

Europe PMC Funders Author Manuscripts

Examples pictures, scale bar=40 μm. *p<0.05 compared to control H_2O_2 treated (n=4), mean ± s.e.m shown in this and all cases. E) Cell death measured by analyzing ATP levels. Treatments as for (D). *p<0.05 compared to control, H_2O_2 treated, n=3. F) Cell death due to 24 h H_2O_2 insult in the face of the indicated treatments, applied 12 h before insult. All activity was terminated *prior* to H_2O_2 exposure (by TTX + MK-801). *p<0.05 compared to control (H_2O_2 treated), n=4. G,H). ROS accumulation following H_2O_2 treatment and in control conditions measured within neurons treated as indicated. Two ROS probes used as indicated. Fluorescence levels were normalized to cell number (as measured using the Celltiter Glo assay, Promega, *p<0.05, n=5).

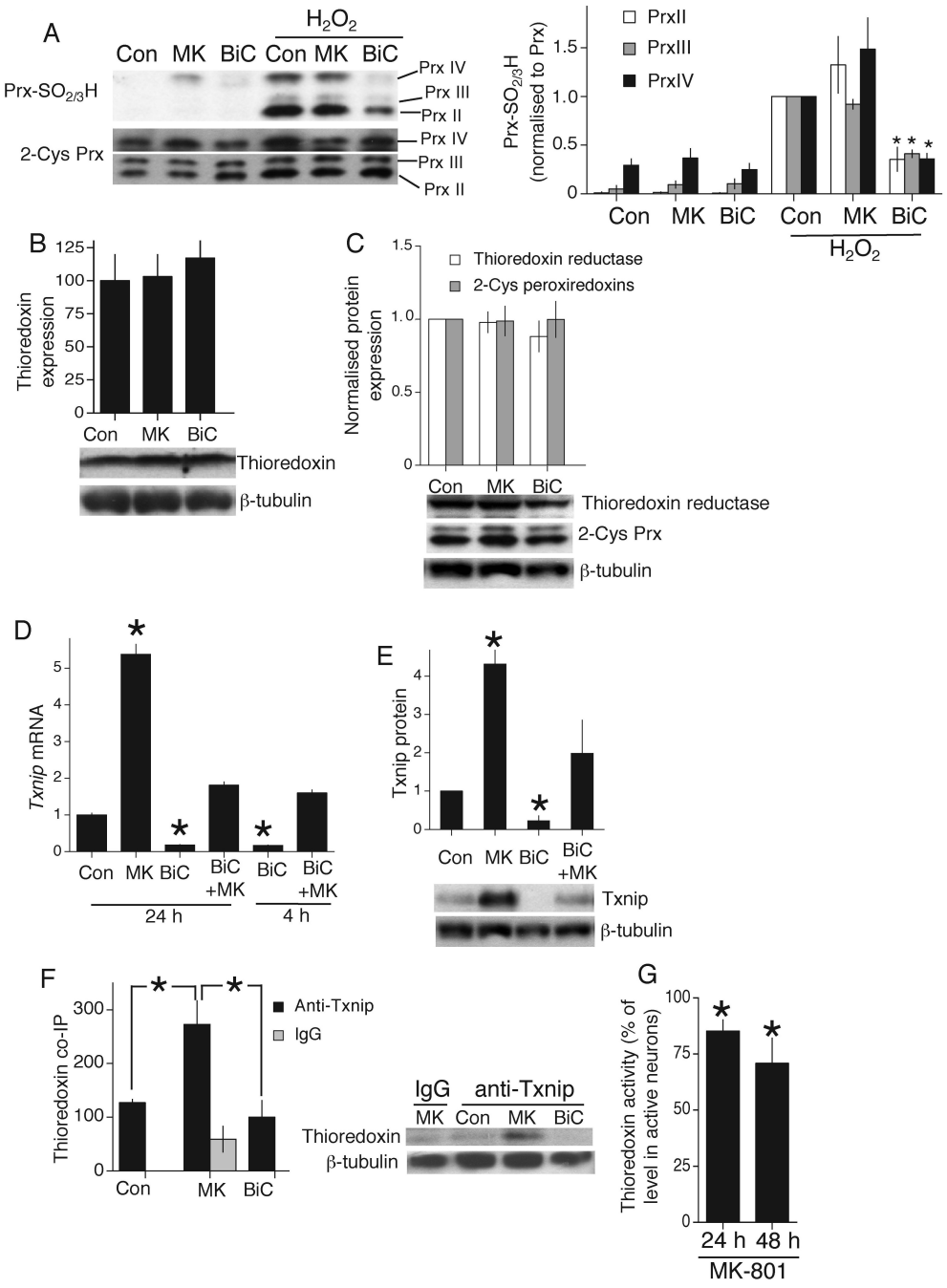

Fig. 2. Synaptic activity prevents the overoxidation of peroxiredoxins in response to an oxidative insult, and negatively regulates the Thioredoxin inhibitor Txnip

A) Western analysis of Prx overoxidation using an anti-Prx$SO_{2/3}$H specific antibody. Analysis normalized to appropriate Prx band intensity. *p<0.05 compared to control, H_2O_2-treated neurons (n=5). Note for upper (PrxIV) band, a higher exposure is often taken to more accurately assess loading (as is the case in the example shown). B,C) Thioredoxin, Thioredoxin reductase and 2-Cys Prx levels analyzed by Western blot after 24 h of the indicated treatments (n=3). D) q-RT-PCR of *Txnip* RNA from rat cortical neurons treated as indicated (this and all subsequent q-RT-PCR data are normalized to Gapdh levels. *p<0.05 compared to control (n=4)). E) Western analysis of Txnip protein expression in response to

the indicated treatments (24 h, *p<0.05 compared to control, n=3). This and all quantitation of Western blots involves normalisation to β-tubulin or other suitable control (such as Akt in the case of Pi-Akt, Prx in the case of $PrxSO_{2/3}H$). F) Co-immunoprecipitation of Thioredoxin with an anti-Txnip antibody in samples from neurons experiencing different levels of synaptic NMDAR activity for 24 h (*p<0.05, n=5). G) Thioredoxin activity (insulin-reducing assay) in neurons treated with MK-801, expressed as a % of the activity observed in BiC/4-AP-treated neurons (*p<0.05 compared to BiC-stimulated neurons, n=6).

Europe PMC Funders Author Manuscripts

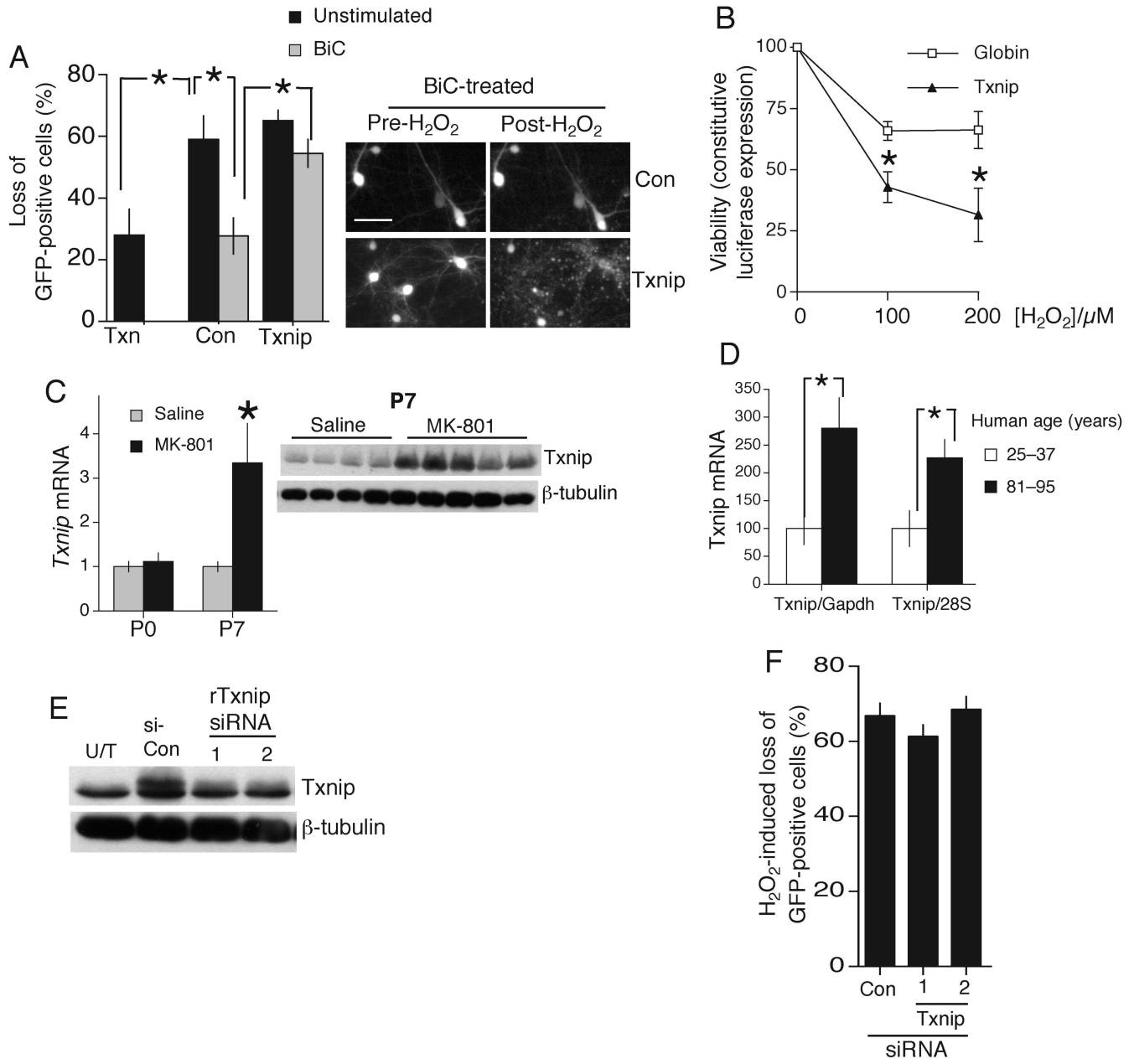

Fig. 3. Txnip and Thioredoxin can regulate neuronal vulnerability to oxidative stress

A) Loss of GFP-positive neurons expressing Txnip, Thioredoxin (Txn) or control plasmid (beta-globin) in the face of 24 h 100 μM H_2O_2. *p<0.05 (n=4). B) Neurons transfected with a constitutively active vector (SV40-Luc) and Txnip or control plasmid, treated with BiC/4-AP prior to oxidative insult for 24 h, followed by luciferase activity measurement *p<0.05 (n=5). C(left) q-RT-PCR of *Txnip* mRNA expression in the murine cortex *in vivo* in response to MK-801 treatment at P0 and P7. *p<0.05 (n=4). C(right) Western blot showing up-regulation of Txnip protein in the cerebral cortex of individual mice *in vivo* by MK-801 treatment of P7 mice. Each lane represents a different mouse. D) RNA from *post-mortem* human frontal cortices was extracted and *TXNIP* mRNA abundance assessed by quantitative RT-PCR. *TXNIP* is shown normalized to *GAPDH* and *28S*, as their expression in the frontal cortex does not change significantly with age49(n=16). E) Neurons transfected with rTxnip

Europe PMC Funders Author Manuscripts

plus control or one of two Txnip-directed siRNAs. Protein harvested at 24 h and subjected to Western analysis for Txnip protein. Untransfected sample (U/T) shown for comparison. F) Loss of GFP-positive neurons transfected with control or one of two *Txnip* siRNAs in the face of 24 h 100 μM H_2O_2. Scale bar 40 μm. Data from 4 independent experiments.

Europe PMC Funders Author Manuscripts

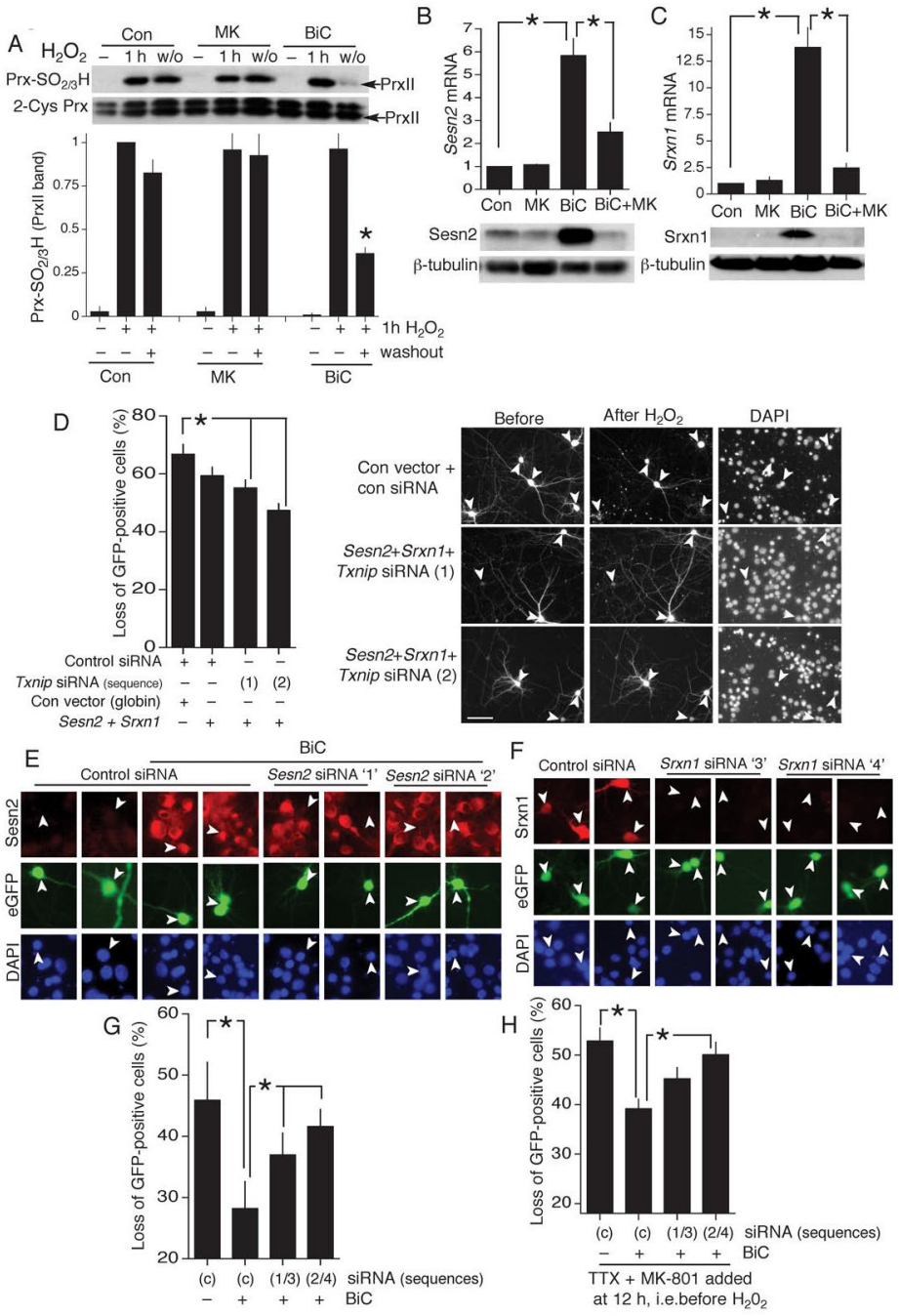

Fig. 4. Synaptic activity promotes reduction of Prx-$SO_{2/3}$H and induces neuroprotective expression of the Prx-$SO_{2/3}$H-reducing genes *Sesn2* and *Srxn1*

A) Recovery of PrxII-$SO_{2/3}$H following a 1 h exposure to high H_2O_2 (200 μM). Neurons stimulated as indicated for 12 h prior to H_2O_2 exposure. Washout period was 16 h (*$p<0.05$ compared to pre-washout level, n=5). B,C) q-RT-PCR of Sestrin2 (*Sesn2, B*) and Sulfiredoxin (*Srxn1, C*) in response to the indicated treatments (BiC stimulation: 4 h). *$p<0.01$ (n=7). Lower panels show regulation of Sesn2 and Srxn1 protein. D) H_2O_2-induced loss of GFP-positive neurons transfected as indicated. Scale bar 60 μm.*$p<0.05$ (one-way ANOVA followed by Fisher's LSD post-hoc test for this and subsequent siRNA experiments, n=4). Right panels show example pictures (arrows indicate transfected neurons

whose fate is studied, Scale bar 60 μm). E) Effect of control- or *Sesn2*-directed siRNA on BiC/4-AP (24 h) induced Sesn2 expression. F) Effect of control- or *Srxn1*-directed siRNA on production of rat Srxn1 driven from an expression vector. G) Effect of knock-down of Sesn2 and Srxn1 on activity-dependent protection against an oxidative insult. Neurons were transfected with control siRNA or one of two pairs of siRNAs which target both *Sesn2* and *Srxn1*. Neurons were stimulated where indicated with BiC/4-AP and then treated with 100 μM H_2O_2. *p<0.05 unpaired T-test (n=4). H) Effect of knock-down of Sesn2 and Srxn1 on long-lasting activity-dependent protection. Experimental details as for (G) except that BiC/4-AP-induced synaptic activity was terminated after 12 h by the addition of TTX + MK-801. After this, the oxidative insult (100 μM H_2O_2) was applied. *p<0.05 (n=6).

Europe PMC Funders Author Manuscripts

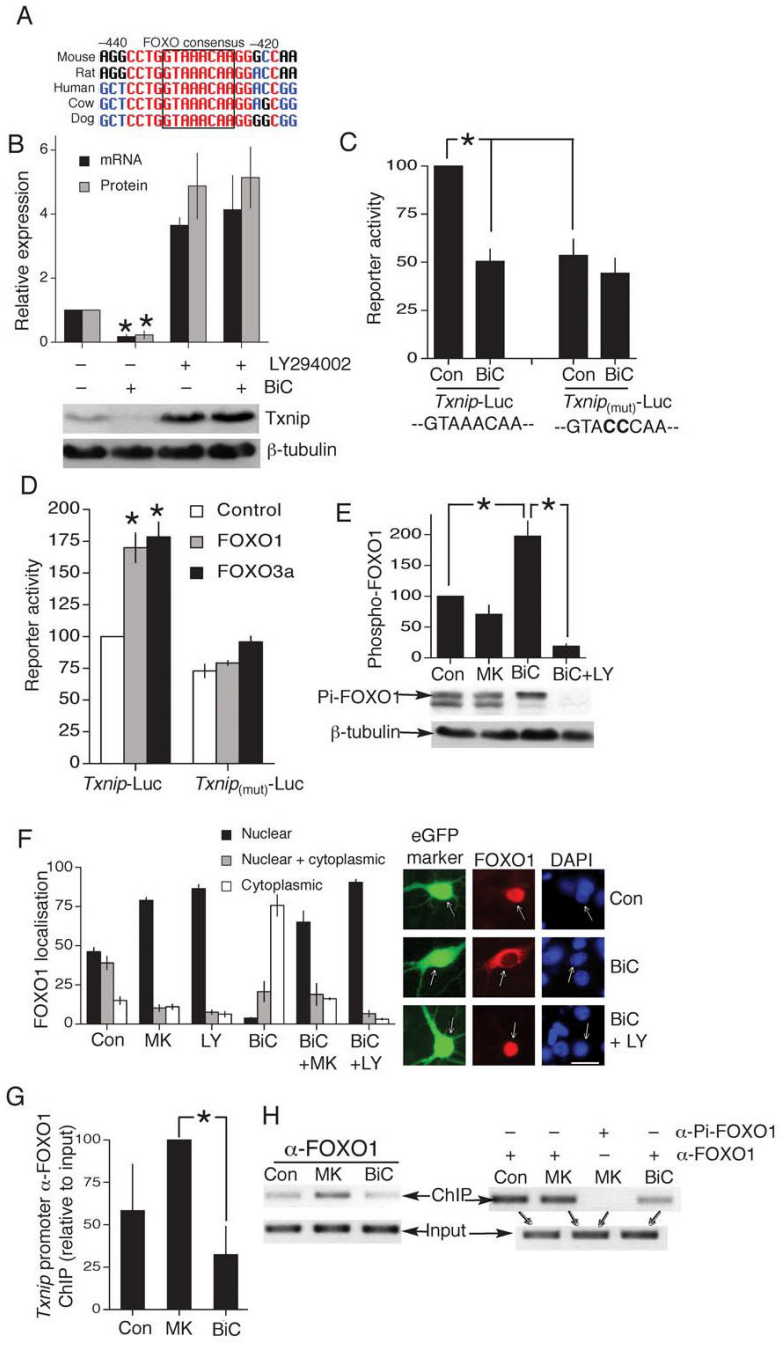

Fig. 5. *Txnip* is a FOXO target gene

A) Schematic showing conservation of a FOXO binding site in the proximal 5′ promoter region of *Txnip*, positions given relative to start of protein coding region (NB. 5′UTR is 222 nt long). B) PI3K inhibition by LY294002 (30 μM) induces *Txnip* expression, and suppression of Txnip protein and mRNA expression by BiC treatment is blocked by LY294002 *p<0.05 compared to control (n=3). C) *Txnip*-Luc and *Txnip*-(mut)-Luc (FOXO site mutated) activity assayed 16 h after the indicated treatments (n=5). In all reporter assays, firefly luciferase based reporter signal is normalized to expression of a cotransfected renilla luciferase control plasmid, pTK-RL. D) *Txnip*-Luc and *Txnip*-(mut)-Luc activity assayed in neurons co-transfected with Control or FOXO expression plasmids. *p<0.05

compared to control plasmid (n=3-5). E) Western analysis of FOXO1 phosphorylation in response to the indicated treatments (30 min stimulation, example Western shown below analysis). *p<0.05 compared to control (n=3). F) Subcellular distribution of transfected myc-tagged FOXO1 analyzed by immunofluorescence (examples on the right; scale bar 30 μm.). G,H) Chromatin immunoprecipitation with an anti-FOXO1 antibody, followed by PCR of the *Txnip* promoter region containing the consensus FOXO binding site (compared to PCR of the input). (G) shows analysis of ChIP band intensity (Normalized to input) relative to MK-801-treated neurons *p<0.05 (n=5). (H) shows example individual ChIP experiments, with (H, right) showing an anti-*phospho*-FOXO1 negative control ChIP.

Europe PMC Funders Author Manuscripts

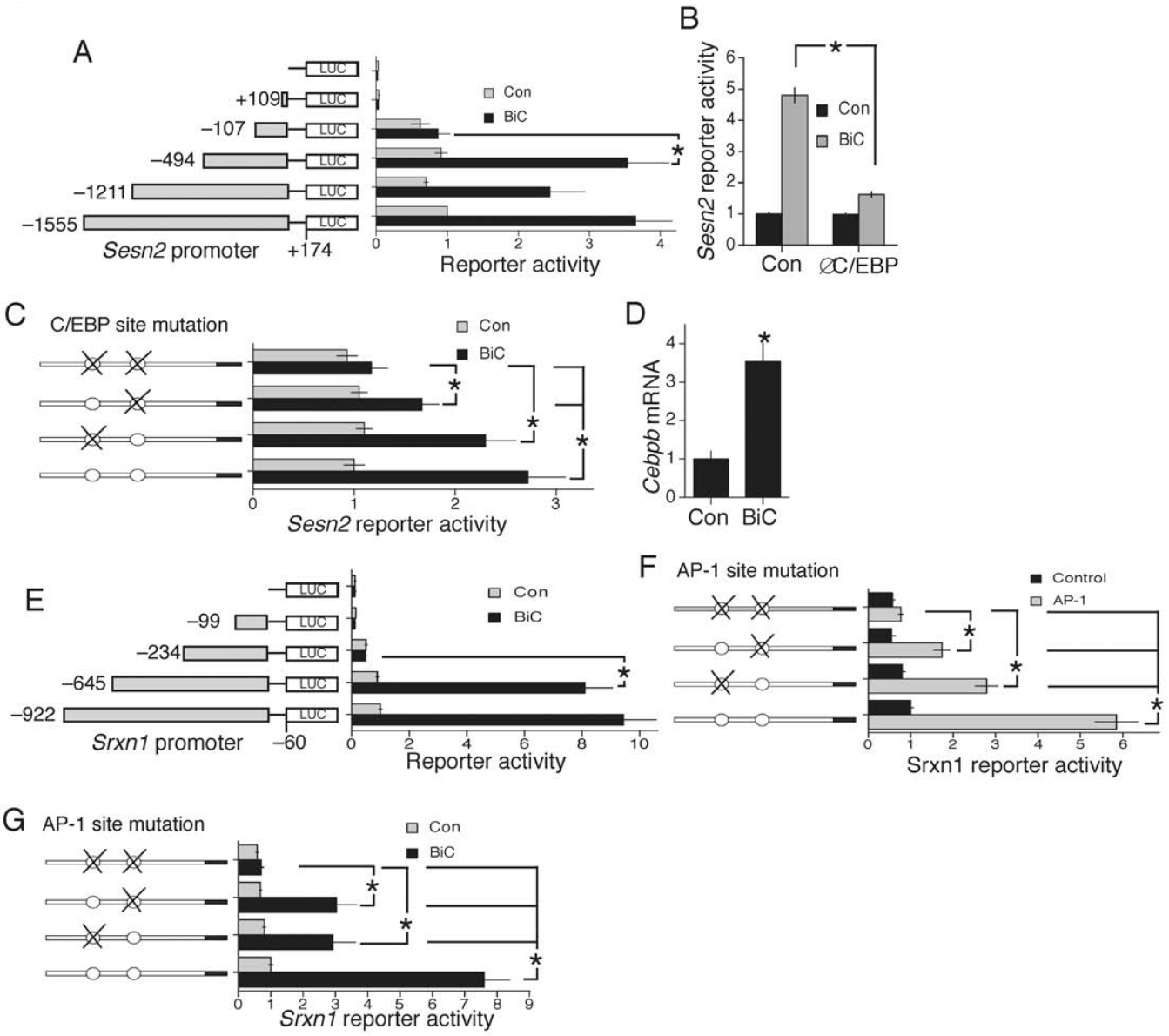

Fig. 6. *Sesn2* is a C/EBP target gene, *Srxn1* is an AP-1 target gene

All experiments performed in cortical neurons. A) Deletion analysis of a luciferase-based reporter of the *Sesn2* promoter. B) Effect of an interfering mutant of C/EBP on activity-dependent induction of the *Sesn2* reporter construct. *p<0.05 compared to control plasmid (n=5). C) Effect of putative C/EBP binding site mutation on activity-dependent induction of the *Sesn2* promoter (distal site ATTTCACACC mutated to ATTTCGGCCC; proximal site TTTGCAGCATC mutated to TTTGCGGCCTC). NB. C/EBP sites have consensus (A/T)TTGCG(C/T)AA(C/T), although quite substantial variations are tolerated50. D) q-RT-PCR of C/EBPβ induction by synaptic activity at 4 h (n=6). E) Deletion analysis of a luciferase-based reporter of the *Srxn1* promoter. F) Effect of AP-1 (cfos+cjun) expression on activity of the *Srxn1* reporter construct, both wild-type and that containing mutations in the two putative AP-1 binding sites (distal site TGAGTCA mutated to TAAGCTT, proximal site TGAGTCA mutated to TGGGCCC). G) Effect of AP-1 site mutation on activity-dependent induction of the *Srxn1* promoter.

Europe PMC Funders Author Manuscripts

Europe PMC Funders Author Manuscripts

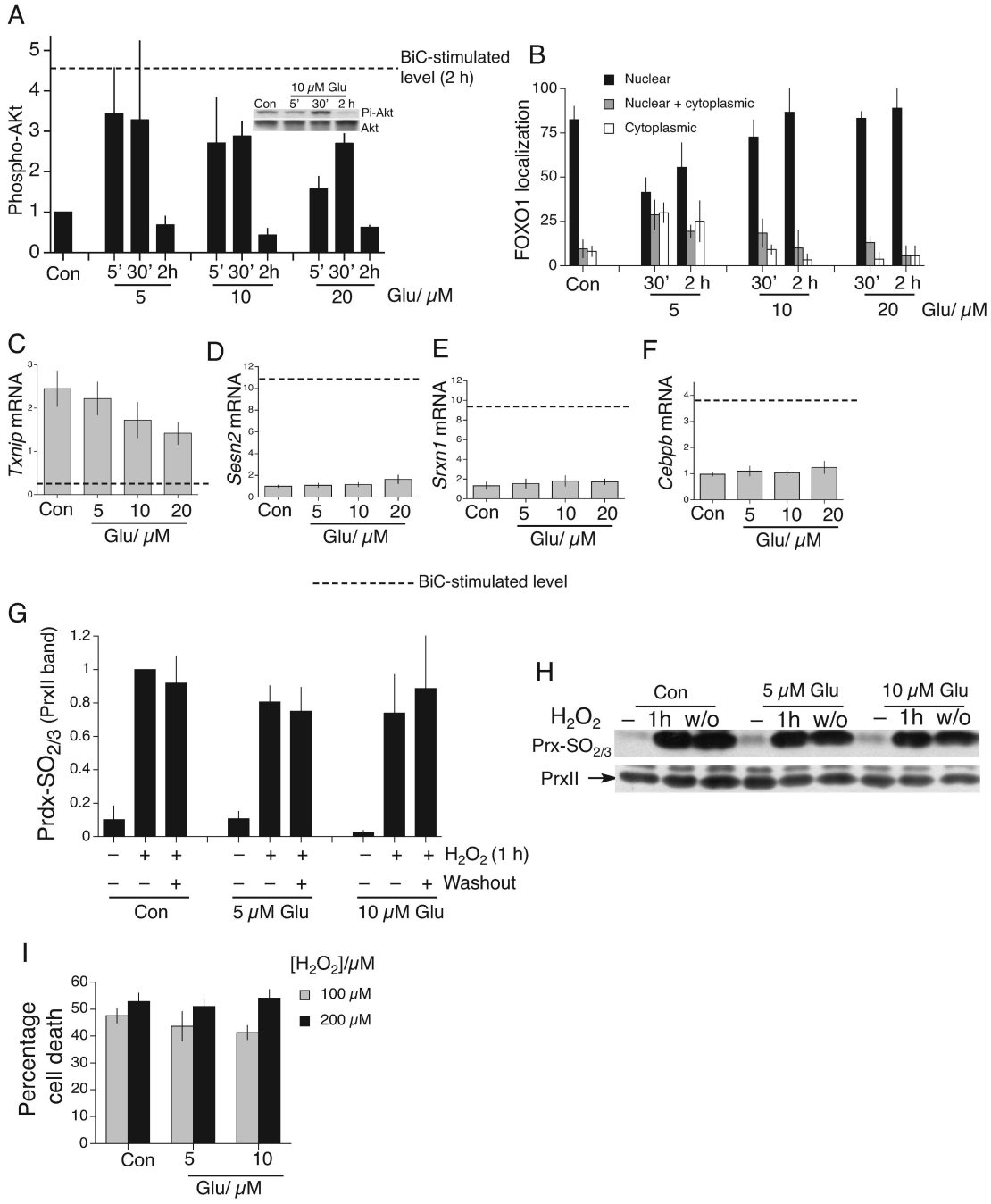

Fig. 7. Extrasynaptic NMDARs do not promote antioxidative effects

A) Phospho-(Serine 473)-Akt kinetics in cortical neurons in response to a range of glutamate concentration (normalized to Akt levels, n=3). The dashed line indicates the level of phospho-Akt induced by BiC/4-AP treatment at 2 h. Example Western also shown. B) Subcellular distribution of transfected myc-tagged FOXO1 analyzed by immunofluorescence, and stimulated as indicated for either 30 min or 2 h (n=3). C-F) q-RT-PCR of the indicated genes in response to a range of glutamate concentrations (4 h stimulation). Dashed line indicates the level of expression following 4 h BiC/4-AP stimulation (n=3). G,H) Lack of recovery of PrxII-$SO_{2/3}$H following a 1 h exposure to high [H_2O_2] (200 μM). Neurons treated with glutamate for 12 h prior to H_2O_2 exposure.

Washout (w/o) period is 16 h. Prx-$SO_{2/3}H$ levels normalized to Prx loading (n=3). I) Cell death due to 24 h H_2O_2 insult in the face of the indicated glutamate treatments, applied 12 h before insult (n=3).

Europe PMC Funders Author Manuscripts

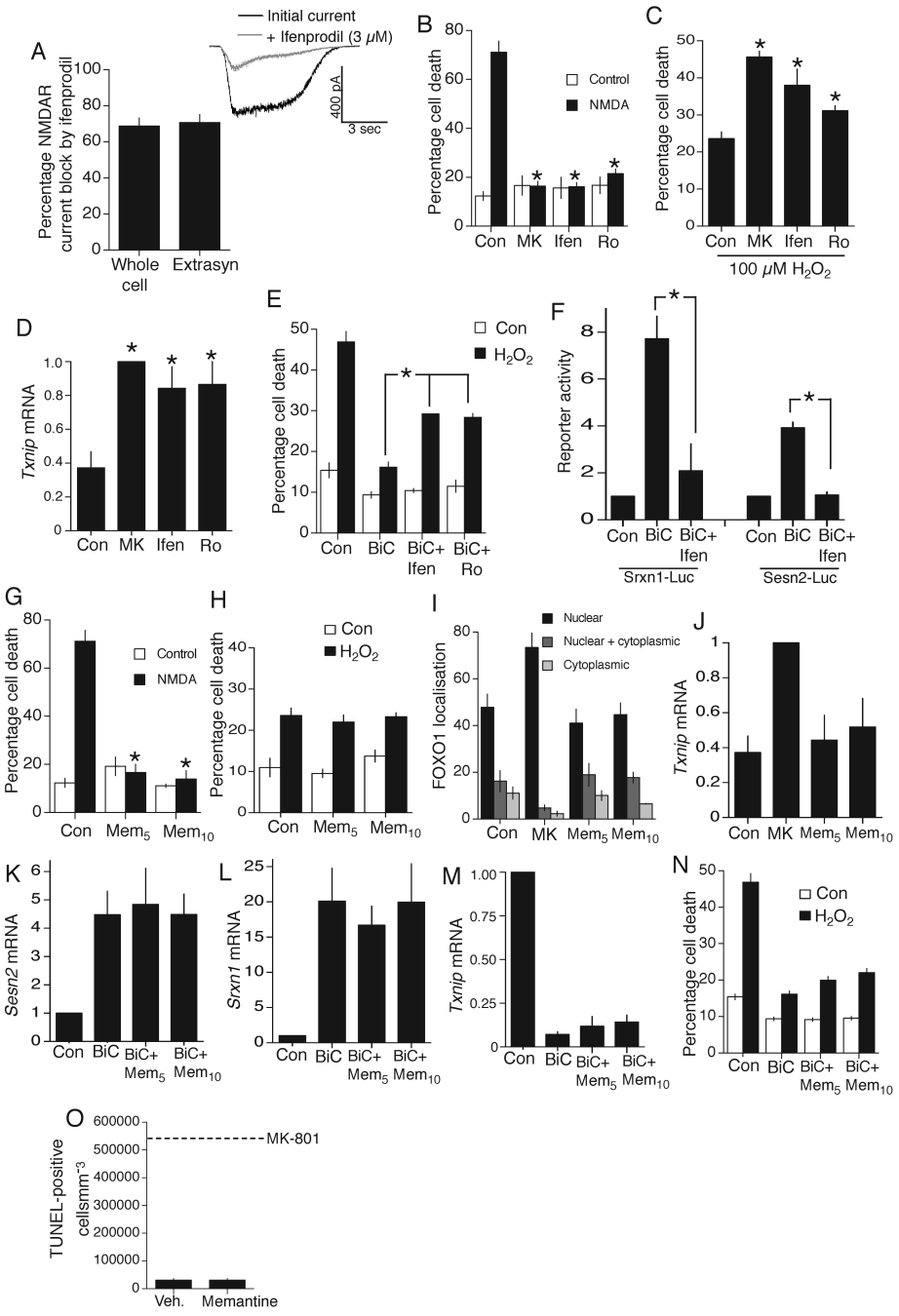

Fig. 8. Memantine, but not NR2B antagonists, discriminate between pro-survival and pro-death NMDAR signaling

A) Ifenprodil (3 μM) sensitivity of whole-cell and extrasynaptic currents (n=8) isolated using the "quantal block" protocol. B) Cell-death induced by 1 h exposure to 50 μM NMDA ± NMDAR antagonists MK-801 (10 μM), ifenprodil (3 μM), Ro 25-6981 (500 nM) *p<0.05 (n=3). C) Cell death due to 24 h H_2O_2 in the face of the indicated treatments, applied 12 h before insult. *p<0.05 (n=4). D) *Txnip* mRNA expression in neurons treated as indicated (24 h). *p<0.05 (n=3). E) Cell death due to 24 h H_2O_2 in the face of the indicated treatments. *p<0.05 (n=3). F) Effect of ifenprodil on BiC/4-AP induction of Sesn2-Luc and Srxn1-Luc. *p<0.05 (n=4). G) Effect of memantine (5 or 10 μM) on NMDA (50 μM)-induced cell

death. *p<0.05 compared to control NMDA treatment (n=3). H) Cell death due to 24 h H_2O_2 insult in the face of the indicated treatments. *p<0.05 (n=3). I) Subcellular distribution of transfected *myc*-tagged FOXO1 analyzed by immunofluorescence. J) *Txnip* mRNA expression in neurons treated for 24 h as indicated. K-M) Effect of memantine on BiC/4-AP-induced changes in *Sesn2* (K), *Srxn1* (L) and *Txnip* (M) expression (n=3). N) Effect of memantine on BiC/4-AP-induced protection against H_2O_2 treatment. O) TUNEL analysis of the cortex of P7 mice subjected to IP-injection of memantine (20 $mgkg^{-1}$) at P6 (for 24 h, n=6). Dotted line indicated the level of death observed with MK-801 injection (Fig. 1a).

Europe PMC Funders Author Manuscripts

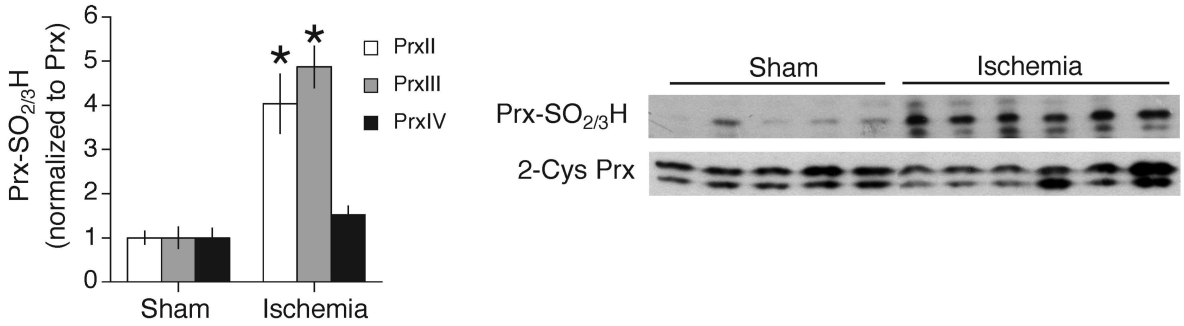

Fig. 9. An ischemic episode, followed by reperfusion, induces overoxidation of peroxiredoxins

Western analysis of Prx-$SO_{2/3}$H formation in homogenate from the MCA territory (cortex and striatum) of mice subjected to 60 min MCAO followed by 3 h reperfusion, compared to the equivalent region from sham-operated mice. Analysis (left) of the Western (right) of 6 ischemic and 5 control samples.